RESEARCH ARTICLE

Neoplasia • Vol. 1, No. 6, December 1999, pp. 518–525 518

Available On-line at http://www.neoplasia.org

Changes in Vascularization of Human Breast Cancer Xenografts Responding to Antiestrogen Therapy[1]

Claus A. Kristensen, Leena M. Hamberg†, George J. Hunter†, Sylvie Roberge*, Diane Kierstead†, Gerald L. Wolf† and Rakesh K. Jain**

*Edwin L. Steele Laboratory of Tumor Biology, Department of Radiation Oncology; †Center for Imaging and Pharmaceutical Research, Massachusetts General Hospital, Harvard Medical School, Boston MA 02114

Abstract

To elucidate the previously suggested vascular effect(s) of antiestrogen therapy, we studied the effect of estrogen withdrawal and tamoxifen on 1) vascular resistance, 2) glucose and oxygen consumption, and 3) vascular density in a perfused breast cancer line (ZR75-1). Furthermore, we examined ZR75-1 tumors by functional CT-scanning (fCT) to determine changes in parameters related to tumor capillary transfer constants and vascular volume fraction in response to antiestrogenic manipulations. The vascular resistance decreased significantly from 42.7 to 20.8 mmHg $\times$ min $\times$ g $\times$ ml^{-1} ($P < .03$) on day 9 after estrogen withdrawal, but not after 9 days of tamoxifen treatment. The estrogen-depleted tumors were significantly smaller than controls on day 9. There was no difference in nutrient consumption or vascular density in any of the experimental groups compared to controls. fCT showed an increase ($P < .03$) in vascular volume fraction during tumor growth, and this parameter was significantly lower after estrogen withdrawal when compared to controls ($P < .05$). Vascular resistance correlated with tumor size ($R = 0.7$, $P < .0001$), indicating that vascular resistance increases during tumor growth. The changes in vascular parameters after estrogen withdrawal indicate a vascular remodeling effect. This inhibition of vascular development by hormone deprivation may have important implications for future planning of multimodal treatment regimens.

Keywords: vascular resistance, estrogen withdrawal, tamoxifen, breast cancer, functional CT-scanning.

Introduction

Induction of vascularization seems to be a limiting step in the development of tumors larger than approximately 1 mm in diameter. At this size, the tumor becomes deprived of oxygen and nutrients, and it has been shown that hypoxia [1] and hypoglycemia [1],[2] can induce release of angiogenic factors (e.g., vascular endothelial growth factor (VEGF)) leading to (in)growth of vessels in tumor tissue. Continuous angiogenesis mediated by VEGF [3], basic fibroblast growth factor (bFGF) [4], or other growth factors [5] is essential for further tumor growth and several anti-angiogenic drugs can inhibit this growth [6–8].

The presence of estrogen receptors and the estrogen-dependent growth of certain human breast cancers have been used in the treatment of this disease for decades. Estrogen withdrawal by ovarian ablation or oral antiestrogen therapy (mainly tamoxifen) are the modalities most widely used; both have improved the prognosis of breast cancer in adjuvant settings [9].

Tamoxifen is a non-steroid competitive inhibitor of the estrogen receptor. However, several investigators have questioned the competitive receptor inhibition as tamoxifen's main mechanism-of-action, because growth-inhibitory effects unrelated to the estrogen receptor have been found. These include stimulation of transforming growth factor (TGF)-β production [10], and binding to specific antiestrogen binding sites other than the estrogen receptor [11],[12]. Furthermore, the metabolic response to estrogen withdrawal differs from the response to tamoxifen treatment in groups of tumors with comparable degree of growth inhibition [13].

In spite of the direct growth inhibition after estrogen withdrawal and/or tamoxifen *in vitro*, it has been proposed that the *in vivo* growth-inhibitory effect of these treatment modalities is partly caused by an anti-angiogenic effect [14–16] which may be unrelated to the receptor status of the tissue [17],[18]. This would explain the 10% to 15% clinical response rate of tamoxifen in estrogen receptor-negative patients [9].

Estrogen-independent tumor growth (i.e., resistance to antiestrogen therapy) can be achieved by FGF-transfection of estrogen-dependent MCF-7 breast cancer cells [19]. These results suggest that the potential anti-angiogenic effect of antiestrogens may be indirect and caused by

Abbreviations: bFGF, basic fibroblast growth factor; $-E_2$, estrogen withdrawal; fCT, functional CT-scanning; VEGF, vascular endothelial growth factor; V_B, vascular volume fraction; VR, vascular resistance.

Address all correspondence to: Claus A. Kristensen, Institute of Molecular Pathology, University of Copenhagen, Box 2713, Frederik V's Vej 11, 5, DK-2100 Copenhagen, Denmark. E-mail: cak@dadlnet.dk

[1]This study was supported by a grant from the US Army (DAMD17-96-1-6282)(R.K.J.), an Outstanding Investigator Grant (R35-CA-56591) from the National Cancer Institute (R.K.J.), and grant from The Danish Medical Research Council (C.A.K.). C.A.K. is a postdoctoral fellow of The Michaelsen Foundation, Denmark.

Received 13 September 1999; Accepted 7 October 1999.

decreased production of angiogenic factors in estrogen-deprived tumor cells.

Understanding the mechanical properties of the tumor microenvironment is of major importance for the design of new treatment strategies [20]. The suggested regulation of vascular development by estrogen/antiestrogen led us to investigate the physiological consequences of hormonal manipulation on tumor vasculature. The estrogen-dependent, estrogen receptor-positive human breast tumor ZR75-1 was used for all experiments, because it has previously been shown to respond to estrogen withdrawal, as well as tamoxifen [13], and because it grows readily as a tissue-isolated tumor. The perfused, tissue-isolated tumor model allowed us to determine the vascular resistance and oxygen/nutrient consumption during continuous estrogen stimulation and after estrogen withdrawal or initiation of tamoxifen therapy. Furthermore, we used a technique recently adapted for studies of human tumor xenografts in nude mice, functional CT-scanning (fCT) [21], for assessment of parameters related to tumor capillary transfer constants (k_1,k_2) and vascular volume fraction (V_B) in response to the applied treatment modalities. CD31 or platelet/endothelial cell adhesion molecule (PECAM) is a sensitive endothelial marker also expressed in myelomonocytic cells in lymph nodes [22]. Staining of tissue sections with antibodies toward CD31 allowed us to relate the tumor vascular density to the data obtained from the *in vivo* studies.

Materials and Methods

Cells and Animals

ZR75-1 human breast cancer cells, obtained from American Type Culture Collection (Rockville, MD), were grown in EMEM (Sigma Chemical Co., St. Louis, MO) with 10% heat-inactivated fetal bovine serum (Sigma). When culture flasks were 90% confluent, cells were scraped off with a rubber policeman, and 2×10^6 cells were injected subcutaneously into the flank of female ovariectomized nude mice carrying a subcutaneous 17β-estradiol pellet (0.72 mg, 60-day release, Innovative Research, Sarasota, CA). For bilateral ovariectomy, the mice were anesthesized with ketamine/xylazine (100/10 mg per kg body weight), a 20-mm longitudinal skin incision was placed over each flank area and the ovaries were isolated through an incision in the abdominal wall. Both ovaries were ligated with a 6-0 silk suture (Ethicon, Somerville, NJ) between the ovary and the distal end of the uterine horn, and the ovaries were removed. Both layers were closed with a 5-0 Ethibond suture (Ethicon). When these tumors had grown to a size of approximately 10 mm in diameter, they were used as donor tissue. All mice were 8 to 10-week-old NCr/Sed-*nu/nu* female athymic mice bred in the Edwin L. Steele Laboratory's animal facility. Institutional guidelines regarding animal welfare were followed.

Tumor Models

Tissue-isolated tumors were used for studies of vascular resistance, oxygen and glucose consumption, lactate production, and vascular density. Due to the demand for a large number of simultaneously growing tumors for the fCT studies, subcutaneously implanted tumors were used for these experiments. It has previously been shown that vascular parameters obtained by fCT do not differ between subcutaneous and tissue-isolated tumors [21].

Subcutaneous Tumors

Nude mice were anesthesized and ovariectomized as described above and a 1-mm^3 chunk of ZR75-1 donor tissue was positioned subcutaneously in the left flank of the animal. During growth, the tumors were measured in two dimensions twice weekly. After 4 to 6 weeks of tumor growth, the mice were split in three groups: In one group, the 17β-estradiol pellet was removed on a day defined as day 0. In the second group, daily s.c. injections of 1 mg tamoxifencitrate (Sigma) in 0.1 ml peanut oil were initiated on day 0. The third group served as continually estrogen-stimulated controls. fCT-scans were performed in all three groups on days -1, 2, and 9.

Tissue-Isolated Tumors

A ZR75-1 tumor slurry was prepared by mincing tumor tissue with a few drops of Hank's buffered salt solution (Sigma). Nude mice were anesthesized with ketamine/xylazine and the left ovary was isolated and removed through incisions in the skin and abdominal wall. Subsequently, the tumor slurry was injected into the ovarian fat pad at the end of the ovarian vascular pedicle, the fat pad with tumor tissue was wrapped in stretched Parafilm and positioned in the subcutaneous space. Thus, the ovarian vessels become the only contributors to the vascularization of the tumor. The right ovary was removed as described in Cells and Animals section and a 17β-estradiol pellet was placed subcutaneously in the back region of the mouse. The Parafilm bag was changed once weekly to allow space for tumor growth and to clean the vascular pedicle for fibrous tissue. After 4 to 6 weeks of tumor growth, the tumors were perfused by cannulation of aorta and vena cava and ligation of aorta and vena cava above the renal vessels and right above the bifurcature. Furthermore, all small vessels going from aorta and to vena cava in the area of cannulation were closed by ligatures. All tumors were perfused with Krebs-Henseleit buffer composed of 118 mM NaCl, 4.7 mM KCl, 1.2 mM KH_2PO_4, 1.2 mM $MgSO_4$, 2.55 mM $CaCl_2$, 0.75 mM papaverin, 11.1 mM glucose, 7000 units/l sodium heparin to avoid coagulation, and 2.5% bovine serum albumin (Sigma). Papaverin is a vasodilator added to avoid vasospasms in the feeding artery during perfusion [23]. The glucose concentration was relatively high (11.1 mM) compared to patients with normoglycemia, but directly comparable to the concentration of 11.5 mM previously found in nude mice [24]. Furthermore, we have previously

found the glucose consumption of perfused melanomas to be constant and independent of flow rate at 11.1 mM [25], which was also desirable for the present experiments. Perfusate flow rate was increased stepwise from 50 to 130 μl/min or until the tumor vein appeared dilated in the surgical microscope. The vascular resistance was calculated from the slope of the linear curve depicting the relationship between perfusate flow rate and arterio-venous pressure drop [26]. For a detailed description of the surgical procedures, see Ref. [27]. Before the perfusion experiments, the mice were split into four groups. In one group, the estradiol pellet was removed 2 days before perfusion. In the second group, the pellet was removed 9 days before perfusion. The mice in the third group were treated with 1 mg tamoxifen-citrate s.c. daily for 9 days before perfusion. The fourth group served as controls; these tumors were perfused during continuous estrogen stimulation. The tissue-isolated tumors were measured once weekly, or when the Parafilm bag was changed.

Functional CT-scanning

Immediately before this procedure, the mice were anesthesized with ketamine/xylazine. Three sequential functional CT studies were performed on three groups of animals; in a control group, in an estrogen withdrawal group and in a group of animals treated with s.c. injections of tamoxifen. The studies were performed on days -1, 2, and 9; the reference day 0 was the day when the treatment was initiated; i.e., either estrogen was withdrawn or first dose of tamoxifen was injected.

fCT imaging was performed under anesthesia, together with a bolus injection of clinically approved iodine CT contrast agent (Renografin 76%, SQUIBB Diagnostics, NJ). After animal preparation and positioning in the CT-scanner, a scout image was obtained, and a multislice study acquired through the tumor. A slice location through the tumor center was then determined for the functional imaging which started before and continued up to 20 minutes after tail vein injection of 150 μl iodine contrast agent.

Initially, fCT data were collected continuously for 30 seconds and reconstructed into images separated by 300 milliseconds [28]. After 30 seconds of continuous imaging, the rate of the data acquisition was changed and images were acquired every 10 seconds for 9 minutes and then every 45 seconds for the next 11 minutes. 120 kVp tube voltage, 150 mA tube current, 2 mm slice thickness, 80 mm reconstruction field, 512×512 image matrix and 1 second 360° X-ray tube rotation time with high resolution imaging mode were used. This provided a nominal voxel size of 0.050 mm^3.

For the quantitation of physiological parameters, vascular volume fraction (V_B) and capillary rate constants (k_1 and k_2), data were transferred from the CT-scanner to a MacIntosh PowerPC 8100/80 work station. A region of interest was placed over the tumor area and a time signal intensity curve was constructed. Similarly, a region of interest was placed over the aorta and an arterial input function obtained. Signal intensities in CT are measured in Hounsfield units (HU) which change linearly as a function of iodine concentration in the tissue [28]. Thus, the time signal intensity curves were converted into time ΔHU curves before fitting into the measured data points a mathematical expression of a two-compartment model:

$$C_T(t) = k_1 \int_0^t \{e^{-k_2(t-\tau)} \cdot CB(\tau)d\tau\} + V_B \cdot CB(t),$$

where $C_T(t)$ is the tissue curve and $CB(t)$ is the blood curve; V_B, k_1, and k_2 are the fitting parameters; V_B is the vascular volume fraction in the tissue of interest, and k_1 and k_2 are the transcapillary rate constants [28].

Glucose Consumption and Lactate Production

Perfusate was sampled from the in- and outlet cannula at each flow rate. Perfusate concentration of glucose and lactate was determined with enzymatic/colorimetric kits (Sigma, Cat. No. 115-A (glucose) and Cat. No. 735-10 (lactate)) and consumption/production was calculated from the arterio-venous concentration differences.

Oxygen Consumption

Samples of perfusate were collected in glass capillary tubes and analyzed in an ABL 300 gas analyzer (Radiometer, Copenhagen, Denmark). Consumption of oxygen was calculated as described previously [25].

Vascular Density

CD31 staining was performed on formalin-fixed, paraffin-embedded tissue-isolated tumors after perfusion. Tissue sections of 4 μm thickness were hydrated in xylene (2×5 min), 99% ethanol (2×5 min), 96% ethanol (3 min), 70% ethanol (3 min), and phosphate-buffered saline (PBS) (5 min). The sections were digested in 0.1% trypsin (Sigma) in PBS at 37°C for 30 min and washed in running deionized water for 10 min. Before and after quenching of endogenous peroxidases in 0.3% hydrogen peroxide in methanol for 30 min, the sections were incubated in 70% ethanol for 5 min. After wash in PBS for 5 min, sections were blocked with three drops of rabbit serum (Vectastain ABC, PK 6104 Rat IgG, Vector Laboratories, Burlingame, CA) in 10 ml PBS for 20 min. The primary MEC 13.3 rat-antimouse PECAM antibody (Pharmingen, San Diego, CA) was added in a concentration of 1:50 in blocking solution (Vectastain ABC) and sections were incubated at 4°C overnight. Primary antibodies were washed off with PBS (3×5 min) and sections were incubated with the biotinylated secondary antibody, rabbit anti-rat IgG (Vectastain ABC) (three drops of rabbit serum and one drop of biotin in 10 ml PBS), for 30 min at room temperature. After 3×5 min PBS wash, the slides were incubated with ABC solution (Vectastain ABC) for 30 min, rinsed and washed in PBS 3×5 min), incubated with peroxidase substrate solution (DAB kit, Vector Laboratories, Burlingame, CA) for 7 min and rinsed in distilled water. Slides were counterstained with haematoxylin, aqueous

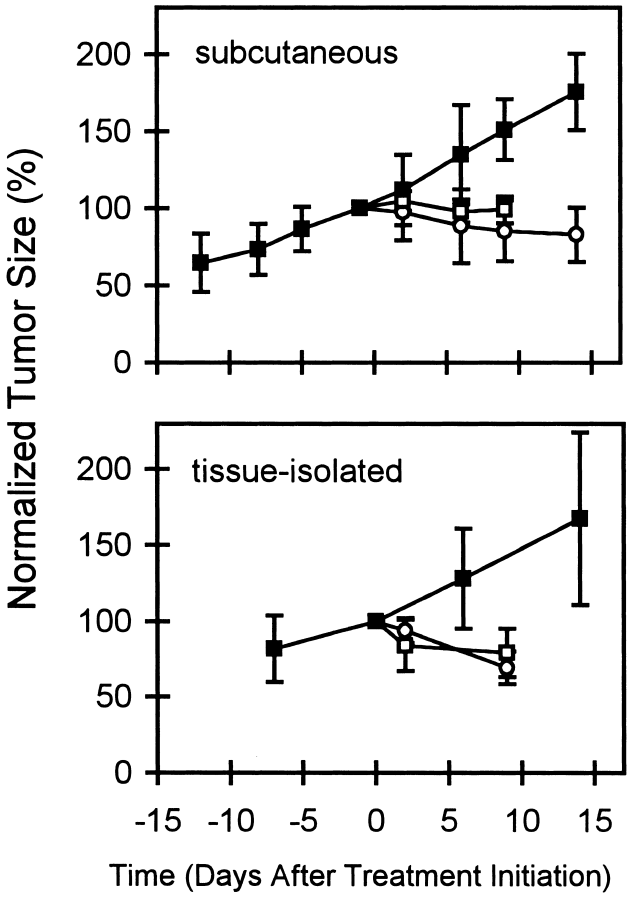

Figure 1. *Growth curves for ZR75-1 subcutaneous (top) and tissue-isolated (bottom) tumors. Tumor measurements were normalized to the size on day −1. The growth inhibition induced by E_2-withdrawal (○) and TAM treatment (□) was significant in both tumor models when compared to controls (■) ($P < .05$, n = 5-7 in each group).*

formula Biomeda, Foster City, CA) for 5 min, rinsed in distilled water for 2 min followed by PBS for 15 min. Finally, the slides were dehydrated and mounted with Permount. Microvessels were quantified by counting the number of brown-staining endothelial cell clusters, clearly separate from adjacent microvessels, tumor cells, and other connective-tissue elements as described by Weidner [29]. The microvessel counts were made on a 0.25-mm^2 field in a non-necrotic area. At least five fields were counted (depending on the tumor size) and the average field count was determined for each tumor.

Statistical Analysis

Differences in tumor growth rates were determined from the α-values extracted from the Gompertz equation of each tumor as described previously [13]. It was not possible to measure the tissue-isolated tumors as frequently as the subcutaneous tumors. Consequently, the α-values of these tumors could not be determined. The growth inhibition of these tumors was determined crudely by normalizing all measures to day 0 (100%) and comparing the change in normalized tumor volume on the day of the experiment. The α-values, as well as all other parameters of control tumors, were compared to values from tumors from experimental groups by a Mann–Whitney test.

Results

Growth of estrogen-stimulated ZR75-1 tumors (controls) and of tumors after estrogen withdrawal and initiation of tamoxifen therapy is shown in Figure 1. In both tumor types (subcutaneous and tissue-isolated), the two treatment modalities induced a significant ($P < .05$) and comparable degree of growth inhibition.

Figure 2 shows a significant decrease in vascular resistance in the $-E_2$ group, whereas tamoxifen treatment did not induce significant changes. Vascular resistance correlated well with tumor size ($R = 0.7$, $P < .0001$, Spearman correlation test) (Figure 2, *bottom*), and since $-E_2$ tumors were significantly smaller than controls ($P < .05$) (Table 1), it is likely, that the low vascular resistance was caused by cessation of tumor growth.

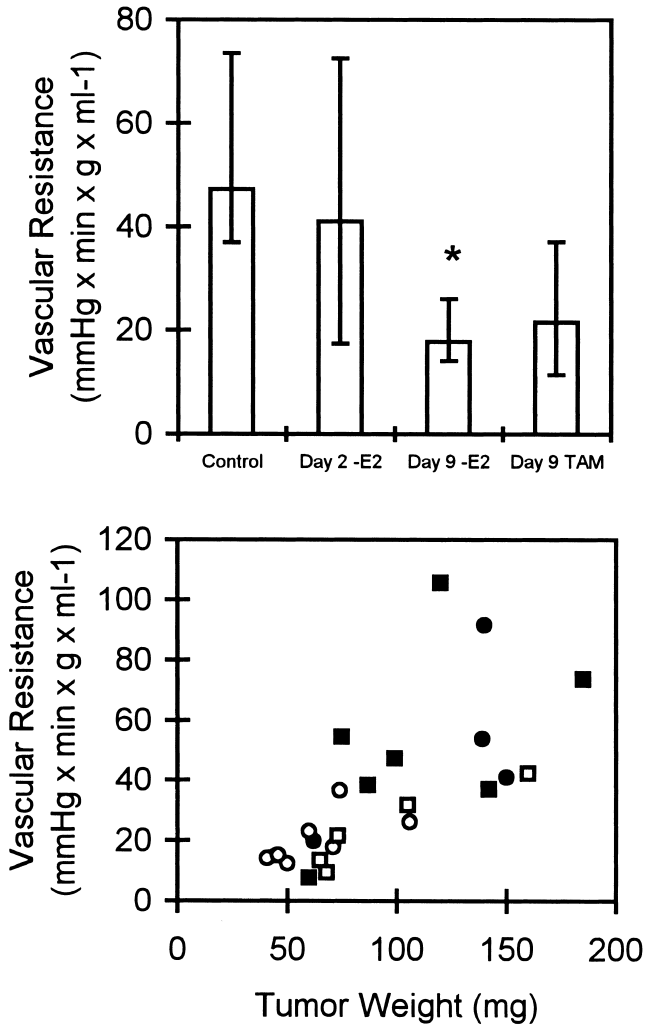

Figure 2. *Top, vascular resistance in each of the three experimental groups was compared to controls. *P < .05, n = 5-7 in each group. Error bars indicate interquartile ranges. Bottom, vascular resistance as a function of tumor weight for controls (■), on days 2 (●) and 9 (○) after estrogen withdrawal and on day 9 after initiation of TAM treatment (□). R = 0.7, P < .0001 (Spearman).*

Table 1. Median tumor weight and glucose, lactate, and oxygen consumption of estrogen-depleted ($-E_2$ days 2 and 9) and tamoxifen (TAM)-treated ZR75-1 tumors. Oxygen consumption is given as percentage of available oxygen (ΔO_2) and as standard oxygen consumption at a delivery rate of 10 μl O_2/min per g. Ranges are given in brackets, *P*-values compared to controls.

	Controls	$-E_2$ (day 2)	$-E_2$ (day 9)	TAM
n	7	5	7	6
Tumor weight (mg)	99 [60 – 185]	140 [45 – 139] *P*=.94	60 [41 – 106] *P*=.021	73 [65 – 160] *P*=.47
ΔGlucose (μmol/min per g)	0.33 [0.17 – 2.07]	1.18 [0.50 – 5.11] *P*=.57	0.79 [0.15 – 1.44] *P*=.39	1.02 [0.4 – 1.49] *P*=.17
ΔLactate (μmol/min per g)	1.48 [0.39 – 2.47]	3.27 [0.33 – 3.53] *P*=.85	0.69 [0.27 – 1.83] *P*=.17	1.02 [0.51 – 1.55] *P*=.37
ΔO_2 (%)	64 [50 – 72]	54 [0.48 – 0.75] *P*=.83	51 [28 – 68] *P*=.16	57 [52 – 65] *P*=.52
St. ΔO_2 (μl/min per g)	7.62 [6.29 – 8.14]	7.12 [5.01 – 8.59] *P*=.58	7.72 [6.27 – 8.87] *P*=.87	7.46 [7.07 – 9.57] *P*=1.00
VD (vessels/field)	5.4 [2.1 – 5.5]	– –	5.1 [3.6 – 8.3] *P*=.44	10.5 [4.2 – 11.3] *P*=.18

Nutrient consumption is shown in Table 1. There was no difference in the consumption of glucose and oxygen or in the production of lactate in the tumor tissue during perfusion.

Table 1 also presents the results of vascular density counts. Vascular density did not change significantly from controls 9 days after estrogen withdrawal or initiation of tamoxifen treatment. There was no significant correlation between glucose consumption and lactate production (R = 0.16, P = .50).

A typical image of the contrast distribution and washout in a subcutaneous ZR75-1 tumor and results from the fCT-scan are shown in Figures 3 and 4. On day 9 after estrogen withdrawal, the vascular volume fraction (V_B) was significantly smaller (P < .03) in $-E_2$ tumors compared to the controls. This difference seemed to be caused mainly by an increase in V_B in controls during tumor growth (P < .03). No significant difference in V_B was observed between the tamoxifen-treated and control tumors. Similarly, no significant differences were observed in the rate constants k_1 and k_2 between the control tumors and either of the treatment groups, estrogen removal or tamoxifen.

Discussion

Antiestrogens and Tumor Growth

The effects of antiestrogen therapy on the tumor growth, and thus on the size of the tumor, were pronounced and comparable in subcutaneous and tissue-isolated tumors (Figure 1). This anti-proliferative effect has previously been attributed to a decreased stimulation of the estrogen receptor in the cytoplasm of tumor cells, leading to decreased DNA synthesis through inhibition of intracellular phosphorylation cascades [30]. It seems generally accepted that antiestrogen treatment leads to apoptosis of estrogen-dependent tumor cells [31–33][34], but the existing data are contradictory and an

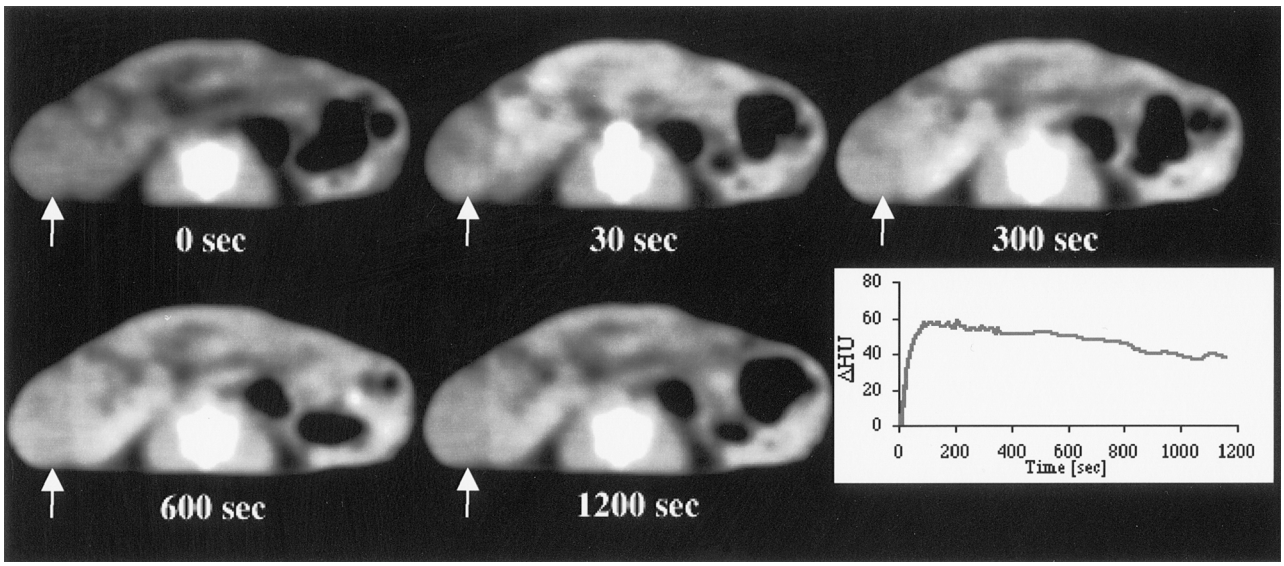

Figure 3. *An example of the contrast agent uptake and washout in a tumor. Images were acquired at the onset of injection and 30, 300, 600, 1200 seconds after intravenous contrast injection. The tumor (white arrow) is seen on the left side of each cross section of the mouse body. Contrast agent uptake is seen as whitening of the tumor tissue. The graph presents temporal changes of ΔHU (and thus the changes in contrast agent concentration) in a tumor. The maximum uptake is reached at 100 seconds after the onset of injection followed by a slow washout.*

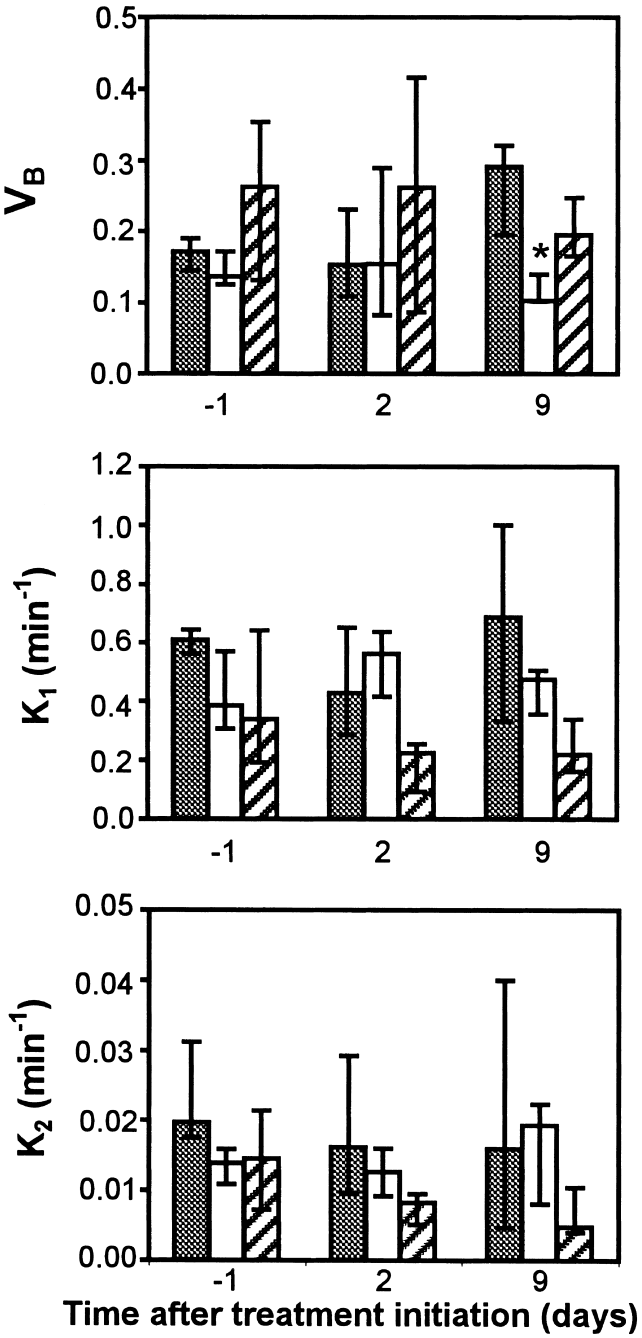

Figure 4. *Changes in V_B, k_1, and k_2 in subcutaneous ZR75-1 tumors after estrogen withdrawal (white columns, n = 5) and TAM treatment initiation (hatched columns, n = 6) compared to controls (grey columns, n = 6) on days −1, 2, and 9. Error bars indicate interquartile ranges. All values were compared to control values at the same time point. *P < .05.*

increased apoptotic index in estrogen-dependent tumors after estrogen withdrawal and/or tamoxifen treatment is not always present [13]. In another study, morphological signs of apoptosis were induced by tamoxifen, but internucleosomal DNA degradation, which is usually a prerequisite for detection of apoptotic cells, was not found [35]. The controversy about the role of apoptosis in response to tumor regression after hormone withdrawal is not unique for breast cancer; in prostate cancer, the relative importance of apoptosis, necrosis, and cell proliferation after testosterone withdrawal differs from patient to patient [36].

It has been demonstrated that antiestrogens inhibit angiogenesis in an *in vivo* chick egg chorioallantoic membrane assay [17], and bFGF- or VEGF-stimulated proliferation of endothelial cells *in vitro* decreases after treatment with the estrogen antagonists tamoxifen, clomifen, nafoxidine, and ICI 182,780 [18]. This effect could not be overcome by addition of estrogen in excess, indicating that the antiangiogenic effect of antiestrogens is unrelated to competitive inhibition of the estrogen receptor [18]. Inhibition of angiogenesis by a mechanism unrelated to the estrogen receptor may explain that 10% to 15% of patients with estrogen receptor-negative tumors respond to tamoxifen treatment [9]. However, estrogen increases the expression of VEGF in rat mammary tumors [15] and in MCF-7 cells [37] and studies in estrogen receptor knockout mice have shown that functional estrogen receptors are necessary for 17β-estradiol-induced angiogenesis [16].

Vascular Parameters

The present study evaluates the effect of antiestrogen therapy on physiological parameters related to tumor angiogenesis and vascularization. In our experiments, estrogen ablation represents a pure antiestrogen effect, whereas tamoxifen is a partial estrogen antagonist with mechanism(s) of action unrelated to inhibition of the estrogen receptor [10][38][39]. Tumor vascular resistance was significantly decreased on day 9 after estrogen withdrawal, but not after tamoxifen treatment (Figure 2, *top*). The decrease in VR was accompanied by a decrease in tumor size. There was a strong correlation ($P < .0001$) between tumor size and vascular resistance (Figure 2, *bottom*), and growth inhibition was probably the reason for lower VR in the estrogen-deprived tumors. An increase in vascular resistance with increasing tumor size corroborates previous studies in rat carcinosarcomas [40] and indicates that these tumors continuously outgrow their vascular supply in spite of constant angiogenesis.

fCT is a new non-invasive method for dynamic measurements of vascular volume fraction and vascular permeability surface area product. The demonstrated increase in vascular volume fraction during estrogen-stimulated tumor growth may indicate an angiogenic effect of estradiol, but it may as well be caused by increased production of angiogenic factors from the proliferating tumor cells. Furthermore, the vascular volume fraction seemed to remain constant after both types of antiestrogen therapy, suggesting that neither of the two treatment modalities was able to decrease the tumor vascularization markedly. The lack of vascular effect of antiestrogen treatment in these experiments is also reflected in the vascular density; there was no significant difference in vascular density between the two experimental groups and controls. As previously discussed, the significant difference in vascular resistance between controls and the $-E_2$ group on day 9 probably reflects a difference in tumor size between the two groups. Consequently, the low vascular resistance after estrogen withdrawal reflects the constancy of the

vascular network when tumor cells are not proliferating, whereas the vascular resistance is increased in the control group due to continuous tumor cell proliferation. The previously detected increase in NTP/P_i [13] cannot be explained by a global increase in tumor perfusion, but can still be due to alterations in microregional perfusion.

It should be kept in mind that the biological intertumoral variation in the values presented in Table 1 and Figure 4 is substantial and some of the methods used have a relatively low reproducibility; these factors may widen the ranges and conceal intratumoral changes.

Antiestrogen Effects on the Vascular Network

Continuous growth stimulation by estrogen increased the vascular resistance and the vascular volume fraction, but did not have any significant impact on the vascular density. How does increased vascular volume fraction lead to *increased* vascular resistance during estrogen-stimulated tumor growth? It has already been shown that tumor vessels are more tortuous and more chaotically distributed than normal vasculature [41] and that regressing vessels gradually become less tortuous [42]. We propose that the increase in vascular volume fraction during estrogen stimulation is secondary to the previously demonstrated increase in VEGF production in estrogen-dependent breast cancer tissue [15][37]. The concomitant increase in vascular tortuosity during tumor growth will *increase* the vascular resistance in spite of a larger vascular bed. Similarly, the lack of estrogen stimulation during regression after estrogen withdrawal decreases the VEGF production and consequently the endothelial proliferation ceases. A marked difference in the vascular network (i.e., straight versus tortuous tumor vessels) has been demonstrated in androgen-dependent Shionogi male mammary tumors during regression after orchiectomy versus continuously androgen-stimulated tumors [43]. Also, apoptosis of endothelial cells was found before apoptosis of Shionogi tumor cells [42]. These data indicate that the anti-angiogenic effect of hormone withdrawal is an indirect effect of reduced production of angiogenic factors in the growth-inhibited tumor cells. This suggestion is further supported by the demonstrated relationship between increased FGF-production and development of estrogen independence [19]. When comparing the data on perfusion and fCT, it should be considered that they were obtained from tissue-isolated and subcutaneous tumors, respectively. Even with this reservation, a cautious comparison can be made, because previous studies have shown that k_1, k_2, and V_B do not differ in the two model systems [21].

Tamoxifen affects the coagulation cascade in humans [44] and antihormonal treatment has been shown to reduce endothelial cell density [14] and induce hypoxia [45] in MCF-7 human breast cancer xenografts. Interestingly, Ruohola *et al.* found that estrogen, as well as tamoxifen alone, induced VEGF mRNA expression [37]. These and several other studies corroborate the idea that tamoxifen has a growth-inhibitory mechanism of action unrelated to competitive inhibition of the estrogen receptor [10–12][13]. This may explain the lack of significant effect of tamoxifen on any of the vascular parameters studied.

In the present experiments, antiestrogen therapy does not seem to reduce the tumor vascularization *per se*— at least not to an extent that increases the vascular resistance beyond the appropriate value for the tumor size. Furthermore, we found no change in oxygen consumption of ZR75-1 tumors after antiestrogen therapy.

In conclusion, estrogen withdrawal may inhibit the indirect angiogenic effect of estrogen-induced bFGF/VEGF release from tumor cell and thereby cease tumor proliferation, but we found no effect of tamoxifen on any of the parameters examined in this study. Still, antiestrogens may prevent the reduction in tumor perfusion (i.e., increase in vascular resistance) that occurs during tumor growth, maintaining an appropriate oxygenation and radiosensitivity of the tumor tissue. This can explain the presumed additive/synergistic effect of antihormonal and radiation therapy [46], as demonstrated *in vivo* in rat [47] and human [48][49] breast cancer.

References

[1] Folkman J (1995). Angiogenesis in cancer, vascular, rheumatoid and other disease. *Nat Med* **1**, 27–31.

[2] Shweiki D, Neeman M, Itin A, and Keshet E (1995). Induction of vascular endothelial growth factor expression by hypoxia and by glucose deficiency in multicell spheroids: implications for tumor angiogenesis. *Proc Natl Acad Sci U S A* **92**, 768–772.

[3] Skobe M, Rockwell P, Goldstein N, Vosseler S, and Fusenig NE 1997). Halting angiogenesis suppresses carcinoma cell invasion. *Nat Med* **3**, 1222–1227.

[4] Rak J, and Kerbel RS (1997). bFGF and tumor angiogenesis— back in the limelight? *Nat Med* **3**, 1083–1084.

[5] Yoshiji H, Harris SR, and Thorgeirsson UP (1997). Vascular endothelial growth factor is essential for initial but not continued *in vivo* growth of human breast carcinoma cells. *Cancer Res* **57**, 3924–3928.

[6] O'Reilly MS, Holmgren L, Shing Y, Chen C, Rosenthal RA, Moses M, Lane WS, Cao Y, Sage EH, and Folkman J (1994). Angiostatin: a novel angiogenesis inhibitor that mediates the suppression of metastases by a Lewis lung carcinoma. *Cell* **79**, 315–328.

[7] O'Reilly MS, Boehm T, Shing Y, Fukai N, Vasios G, Lane WS, Flynn E, Birkhead JR, Olsen BR, and Folkman J (1997). Endostatin: an endogenous inhibitor of angiogenesis and tumor growth. *Cell* **88**, 277–285.

[8] Gradishar WJ (1997). An overview of clinical trials involving inhibitors of angiogenesis and their mechanism of action. *Invest New Drugs* **15**, 49–59.

[9] Early Breast Cancer Trialists' Collaborative Group (1992). Systemic treatment of early breast cancer by hormonal, cytotoxic, or immune therapy: Part 1. *Lancet* **339**, 1–15.

[10] Knabbe C, Lippman ME, Wakefield LM, Flanders KC, Kasid A, Derynck R, and Dickson RB (1987). Evidence that transforming growth factor-β is a hormonally regulated negative growth factor in human breast cancer cells. *Cell* **48**, 417–428.

[11] Faye J-C, Jozan S, Redeuilh G, Baulieu E-E, and Bayard F (1983). Physicochemical and genetic evidence for specific antiestrogen binding sites. *Proc Natl Acad Sci U S A* **80**, 3158–3162.

[12] Murphy LC, and Sutherland RL (1981). A high-affinity binding site for the antioestrogens, tamoxifen and CI 628, in immature rat uterine cytosol which is distinct from the oestrogen receptor. *J Endocrinol* **91**, 155–161.

[13] Kristensen CA, Kristjansen PEG, Brünner N, Quistorff B, and Spang-Thomsen M (1995). Growth inhibition in response to estrogen withdrawal and tamoxifen therapy of human breast cancer xenografts evaluated by *in vivo* ^{31}P MRS, creatine kinase activity, and apoptotic index. *Cancer Res* **55**, 4146–4150.

[14] Furman-Haran E, Maretzek AF, Goldberg I, Horowitz A, and Degani H (1994). Tamoxifen enhances cell death in implanted MCF7

breast cancer by inhibiting endothelium growth. *Cancer Res* **54**, 5511–5514.

[15] Nakamura J, Savinov A, Lu Q, and Brodie A (1996). Estrogen regulates vascular endothelial growth/permeability factor expression in 7,12-dimethylbenz(*a*)anthracene-induced rat mammary tumors. *Endocrinology* **137**, 5589–5596.

[16] Johns A, Freay AD, Fraser W, Korach KS, and Rubanyi GM (1996). Disruption of estrogen receptor gene prevents 17β estradiol-induced angiogenesis in transgenic mice. *Endocrinology* **137**, 4511–4513.

[17] Gagliardi A, and Collins DC (1993). Inhibition of angiogenesis by antiestrogens. *Cancer Res* **53**, 533–535.

[18] Gagliardi AR, Hennig B, and Collins DC (1996). Antiestrogens inhibit endothelial cell growth stimulated by angiogenic growth factors. *Anticancer Res* **16**, 1101–1106.

[19] McLeskey SW, Zhang L, El-Ashry D, Trock BJ, Lopez CA, Kharbanda S, Tobias CA, Lorant LA, Hannum RS, Dickson RB, and Kern, FG (1998). Tamoxifen-resistant fibroblast growth factor-transfected MCF-7 cells are cross-resistant *in vivo* to the antiestrogen ICI 182,780 and two aromatase inhibitors. *Clin Cancer Res* **4**, 697–711.

[20] Fagrell B, and Intaglietta M (1997). Microcirculation: its significance in clinical and molecular medicine. *J Int Med* **241**, 349–362.

[21] Hamberg LM, Kristjansen PEG, Hunter GJ, Wolf GL, and Jain RK (1994). Spatial heterogeneity in tumor perfusion measured with functional computed tomography at 0.05 μl resolution. *Cancer Res* **54**, 6032–6036.

[22] Horak ER, Leek R, Klenk N, Lejeune S, Smith K, Stuart N, Greenall M, Stepniewska K, and Harris AL (1992). Angiogenesis, assessed by platelet/endothelial cell adhesion molecule antibodies, as indicator of node metastases and survival in breast cancer. *Lancet* **340**, 1120–1124.

[23] Sevick EM, and Jain RK (1989). Geometric resistance to blood flow in solid tumors perfused *ex vivo*: effects of tumor size and perfusion pressure. *Cancer Res* **49**, 3506–3512.

[24] Kristensen CA, Askenasy N, Jain RK, and Koretsky AP (1999). Creatine and cyclocreatine treatment of human colon adenocarcinoma xenografts: ^{31}P and ^{1}H magnetic resonance spectroscopic studies. *Br J Cancer* **79**, 278–285.

[25] Kristensen CA, Roberge S, and Jain RK (1997). Effect of tumor necrosis factor α on vascular resistance, nitric oxide production, and glucose and oxygen consumption in perfused tissue-isolated human melanoma xenografts. *Clin Cancer Res* **3**, 319–324.

[26] Kristjansen PEG, Brown TJ, Shipley LA, and Jain RK (1996). Intratumor pharmacokinetics, flow resistance, and metabolism during gemcitabine infusion in *ex vivo* perfused human small cell lung cancer. *Clin Cancer Res* **2**, 359–367.

[27] Kristjansen PEG, Roberge S, Lee I, and Jain RK (1994). Tissue-isolated human tumor xenografts in athymic nude mice. *Microvasc Res* **48**, 389–402.

[28] Groothuis DR, Lapin GD, Vriesendorp FJ, Mikhael MA, and Patlak CS (1991). A method to quantitatively measure transcapillary transport of iodinated compounds in canine brain tumors with computed tomography. *J Cereb Blood Flow Metab* **11**, 939–948.

[29] Weidner N (1995). Current pathologic methods for measuring intratumoral microvessel density within breast carcinoma and other solid tumors. *Breast Cancer Res Treat* **36**, 169–180.

[30] el Ashry D, and Lippman ME (1994). Molecular biology of breast carcinoma. *World J Surg* **18**, 12–20.

[31] Kyprianou N, English HF, Davidson NE, and Isaacs JT (1991). Programmed cell death during regression of the MCF-7 human breast cancer following estrogen ablation. *Cancer Res* **51**, 162–166.

[32] Wärri AM, Huovinen RL, Laine AM, Martikainen PM, and Härkönen PL (1993). Apoptosis in toremifene-induced growth inhibition of human breast cancer cells *in vivo* and *in vitro*. *J Natl Cancer Inst* **85**, 1412–1418.

[33] Cameron DA, Ritchie AA, Langdon S, Anderson TJ, and Miller WR (1997). Tamoxifen induced apoptosis in ZR-75 breast cancer xenografts antedates tumour regression. *Breast Cancer Res Treat* **45**, 99–107.

[34] Ellis PA, Saccani-Jotti G, Clarke R, Johnston SR, Anderson E, Howell A, A'Hern R, Salter J, Detre S, Nicholson R, Robertson J, Smith IE, and Dowsett M (1997). Induction of apoptosis by tamoxifen and ICI 182780 in primary breast cancer. *Int J Cancer* **72**, 608–613.

[35] Otto AM, Paddenberg R, Schubert S, and Mannherz HG (1996). Cell-cycle arrest, micronucleus formation, and cell death in growth inhibition of MCF-7 breast cancer cells by tamoxifen and cisplatin. *J Cancer Res Clin Oncol* **122**, 603–612.

[36] Colecchia M, Frigo B, Del Boca C, Guardamagna A, Zucchi A, Colloi D, and Leopardi O (1997). Detection of apoptosis by the TUNEL technique in clinically localised prostatic cancer before and after combined endocrine therapy. *J Clin Pathol* **50**, 384–388.

[37] Ruohola JK, Valve EM, Karkkainen MJ, Joukov V, Alitalo K, and Harkonen PL (1999). Vascular endothelial growth factors are differentially regulated by steroid hormones and antiestrogens in breast cancer cells. *Mol Cell Endocrinol* **149**, 29–40.

[38] Fuqua S.A.W. (1994). Estrogen receptor mutagenesis and hormone resistance. *Cancer* **74**, 1026–1029.

[39] Pavlik EJ, Nelson K, Srinivasan S, Powell DE, Kenady DE, DePriest PD, Gallion HH, and van Nagell JR, Jr (1992). Resistance to tamoxifen with persisting sensitivity to estrogen: possible mediation by excessive antiestrogen binding site activity. *Cancer Res* **52**, 4106–4112.

[40] Sensky PL, Prise VE, Tozer GM, Shaffi KM, and Hirst DG. Resistance to flow through tissue-isolated transplanted rat tumours located in two different sites. *Br J Cancer* **67**, 1337–1341.

[41] Less JR, Skalak TC, Sevick EM, and Jain RK (1991). Microvascular architecture in a mammary carcinoma: branching patterns and vessel dimensions. *Cancer Res* **51**, 265–273.

[42] Jain RK, Safabakhsh N, Sckell A, Chen Y, Jiang P, Benjamin L, Yuan F, and Keshet E (1998). Endothelial cell death, angiogenesis and microvascular function following castration in an androgen dependent tumor: role of vascular endothelial growth factor. *Proc Natl Acad Sci U S A* **95**, 10820–10825.

[43] Gazit Y, Baish JW, Safabakhsh N, Leunig M, Baxter LT, and Jain RK (1997). Fractal characteristics of tumor vascular architecture during tumor growth and regression. *Microcirculation* **4**, 395–402.

[44] Pemberton KD, Melissari E, and Kakkar VV (1993). The influence of tamoxifen on the main natural anticoagulants and fibrinolysis. *Blood Coagulation, Fibrinolysis* **4**, 935–942.

[45] Evans SM, Koch CJ, Laughlin KM, Jenkins WT, Van Winkle T, and Wilson DF (1997). Tamoxifen induces hypoxia in MCF-7 xenografts. *Cancer Res* **57**, 5155–5161.

[46] Tannock IF (1996). Treatment of cancer with radiation and drugs. *J Clin Oncol* **14**, 3156–3174.

[47] Kantorowitz DA, Thompson HJ, and Furmanski P (1993). Effect of conjoint administration of tamoxifen and high-dose radiation on the development of mammary carcinoma. *Int J Radiat Oncol Biol Phys* **26**, 89–94.

[48] Cooke AL, Perera F, Fisher B, Opeitum A, and Yu N (1995). Tamoxifen with and without radiation after partial mastectomy in patients with involved nodes. *Int J Radiat Oncol Biol Phys* **31**, 777–781.

[49] Zietman AL, Nakfoor BM, Prince EA, and Gerweck LE (1997). The effect of androgen deprivation and radiation therapy on an androgen sensitive murine tumor: an *in vitro* and *in vivo* study. *Cancer J Sci Am* **3**, 31–36.